Published OnlineFirst November 14, 2011; DOI: 10.1158/0008-5472.CAN-11-1515

Intermittent Administration of MEK Inhibitor GDC-0973 plus PI3K Inhibitor GDC-0941 Triggers Robust Apoptosis and Tumor Growth Inhibition

Klaus P. Hoeflich[1], Mark Merchant[1], Christine Orr[1], Jocelyn Chan[1], Doug Den Otter[1], Leanne Berry[1], Ian Kasman[1], Hartmut Koeppen[1], Ken Rice[2], Nai-Ying Yang[1], Stefan Engst[2], Stuart Johnston[2], Lori S. Friedman[1], and Marcia Belvin[1]

Abstract

Combinations of MAP/ERK kinase (MEK) and phosphoinositide 3-kinase (PI3K) inhibitors have shown promise in preclinical cancer models, leading to the initiation of clinical trials cotargeting these two key cancer signaling pathways. GDC-0973, a novel selective MEK inhibitor, and GDC-0941, a class I PI3K inhibitor, are in early stage clinical trials as both single agents and in combination. The discovery of these selective inhibitors has allowed investigation into the precise effects of combining inhibitors of two major signaling branches downstream of RAS. Here, we investigated multiple biomarkers in the mitogen-activated protein kinase (MAPK) and PI3K pathway to search for points of convergence that explain the increased apoptosis seen in combination. Using washout studies *in vitro* and alternate dosing schedules in mice, we showed that intermittent inhibition of the PI3K and MAPK pathway is sufficient for efficacy in BRAF and KRAS mutant cancer cells. The combination of GDC-0973 with the PI3K inhibitor GDC-0941 resulted in combination efficacy *in vitro* and *in vivo* via induction of biomarkers associated with apoptosis, including Bcl-2 family proapoptotic regulators. Therefore, these data suggest that continuous exposure of MEK and PI3K inhibitors in combination is not required for efficacy in preclinical cancer models and that sustained effects on downstream apoptosis biomarkers can be observed in response to intermittent dosing. *Cancer Res; 72(1); 210–9. ©2011 AACR.*

Introduction

The MAP/ERK kinase (MEK) signaling cascade transduces multiple proliferation and differentiation signals within the cell via activation of the RAS GTPase and subsequent sequential activation of RAF, MEK, and extracellular signal–regulated kinase (ERK). Aberrant regulation of this pathway contributes to many hallmarks of cancer cells, including uncontrolled proliferation, invasion, metastasis, angiogenesis, and evasion of apoptosis (1, 2). Inhibition of MEK is a promising strategy in the development of oncology therapeutics to control the growth of tumors that are dependent on aberrant MEK pathway signaling (3–5). The MEK pathway is upregulated in a large fraction of tumors, in part, due to mutation of several components of the pathway. Oncogenic-activating mutations have been identified in KRAS (22% of all cancers), NRAS (8%), HRAS (3%), and BRAF (20%; COSMIC database; ref. 6). Activating BRAF mutations, the majority of which are a single amino acid substitution (V600E) in the activation loop of the kinase (6, 7), are prevalent in malignant melanomas (66%) and are also found in colon cancer (15%) and thyroid papillary carcinoma (27%). Cancer cells transformed by BRAF V600E are highly sensitive to MEK1/2 inhibition (4, 8). In addition to RAS and RAF mutations, many tumors are activated by amplification or overexpression of upstream pathway components. Therefore, MEK1/2 inhibitors may have broad utility in tumors with mitogen-activated protein kinase (MAPK) pathway alterations.

PI3K–AKT pathway activation has been implicated in several types of cancer (9, 10). Activating and transforming mutations in the p110α subunit of phosphoinositide 3-kinase (PI3K) are commonly found in multiple tumor types (11–13). In addition, the pathway is activated in numerous types of cancer by receptor tyrosine kinase (RTK) signaling, RAS mutations, or the loss of the phosphatase PTEN (10).

Targeting either of these pathways individually can attenuate signaling and has been shown to be efficacious in animal models (14, 15). However, in some tumors, cell proliferation and survival are driven through multiple effector pathways, such as in tumors with concurrent activation of the RAS and PI3K pathways, as is seen in a subset of melanoma, lung, and

Authors' Affiliations: [1]Genentech, Inc. and [2]Exelixis, Inc., South San Francisco, California

Note: Supplementary data for this article are available at Cancer Research Online (http://cancerres.aacrjournals.org/).

K.P. Hoeflich and M. Merchant contributed equally to this work.

Current address for S. Engst: Cytokinetics, Inc., South San Francisco, California.

Corresponding Author: Marcia Belvin, Genentech Inc., 1 DNA Way, South San Francisco, CA 94080. Phone: 650-467-7346; Fax: 650-225-1411; E-mail: mbelvin@gene.com

doi: 10.1158/0008-5472.CAN-11-1515

Published OnlineFirst November 14, 2011; DOI: 10.1158/0008-5472.CAN-11-1515

colorectal cancers. Targeting both of these pathways is significantly more efficacious in preclinical models than targeting either pathway alone (15, 16). Pathway feedback, resulting in activation of parallel pathways in response to targeted inhibitors, can also contribute to combination efficacy (15–18).

GDC-0973 is a novel small-molecule inhibitor of MEK that is potent and highly selective. The results presented here show that when GDC-0973 is combined with the PI3K inhibitor GDC-0941 in cancer models, it results in combination efficacy *in vitro* and *in vivo* via induction of biomarkers associated with apoptosis, including Bcl-2 family proapoptotic regulators (19). These findings suggest that intermittent dosing regimens may be efficacious for combinations of MEK and PI3K inhibitors in the clinic and that sustained exposure to inhibitors may not be required for maximal combination efficacy.

Materials and Methods

Cell line single-nucleotide polymorphism fingerprinting

Single-nucleotide polymorphism (SNP) genotyping was carried out for all cell lines except 888MEL, DU-145.X1, and NCI-H520.X1. Cells were obtained from American Type Culture Collection. Cell line identity was verified by high throughput SNP genotyping using Illumina Golden gate multiplexed assays. SNPs were selected on the basis of minor allele frequency and presence on commercial genotyping platforms. SNP profiles were compared with SNP calls from the Sanger database to confirm ancestry for the following cell lines: 22Rv1, A2058, A375, A549, Calu-6, FaDu, HCT-116, LoVo, MiaPaCa-2, NCI-H2122, NCI-H441, NCI-H460, and SKOV-3.

Cell viability assays

GDC-0941 and GDC-0973 were obtained from the Chemistry Department at Genentech, Inc. Cell viability and synergy assays were conducted as previously described (18, 20). To ascertain the role of Bim in apoptosis mediated by GDC-0941 and GDC-0973, siRNA oligonucleotides were obtained from Dharmacon RNAi Technologies. The quantity of cytoplasmic histone-associated DNA fragments was quantified by the Cell Death Detection ELISA Plus kit from Roche according to the manufacturer's instructions.

Immunoblotting

To prepare extracts, cells were washed once with cold PBS and lysed in 1× Cell Extraction Buffer (Biosource) as described by the manufacturer. For frozen tumor samples, tumors were pulverized on dry ice by a small Bessman tissue pulverizer (Spectrum Laboratories) and prepared as described by the manufacturer.

Antibodies to cleaved PARP, phospho-AKT (p-AKT), phospho-ERK (p-ERK), pS6, Bim, and cyclin D1 were obtained from Cell Signaling. The β-actin and glyceraldehyde-3-phosphate dehydrogenase (GAPDH) antibodies were obtained from Sigma. Specific antigen–antibody interaction was detected with an horseradish peroxidase (HRP)-conjugated secondary antibody IgG using ECL detection reagents (Amersham Biosciences). The p-ERK and total-ERK (t-ERK) band intensities were quantified by the LI-COR Odyssey immunoblotting system.

Pharmacodynamic assays

Frozen tumors were pulverized on dry ice using a small Bessman tissue pulverizer (Spectrum Laboratories) and prepared according to the manufacturer. For subsequent Western blot analysis, proteins were resolved by 4% to 12% SDS-PAGE and transferred to nitrocellulose membranes (Millipore Corporation) and immunoblotting carried out as described earlier.

Tumor and body weight measurement

Tumor volumes were determined with digital calipers (Fred V. Fowler Company, Inc.) using the formula $(L \times W \times W)/2$. Tumor growth inhibition (TGI) was calculated as the percentage of the area under the fitted curve (AUC) for the respective dose group per day in relation to the vehicle, such that $\%TGI = 100 \times [1 - (AUC_{treatment}/d)/(AUC_{vehicle}/d)]$. Curve fitting was applied to $\log_2$-transformed individual tumor volume data using a linear mixed-effects model with the R package nlme, version 3.1-97 in R v2.12.0.

Results

GDC-0973 and GDC-0941 are selective inhibitors of MEK and PI3K

GDC-0973 is a potent and highly selective inhibitor of MEK (Fig. 1A), with a biochemical IC_{50} value of 4.2 nmol/L against

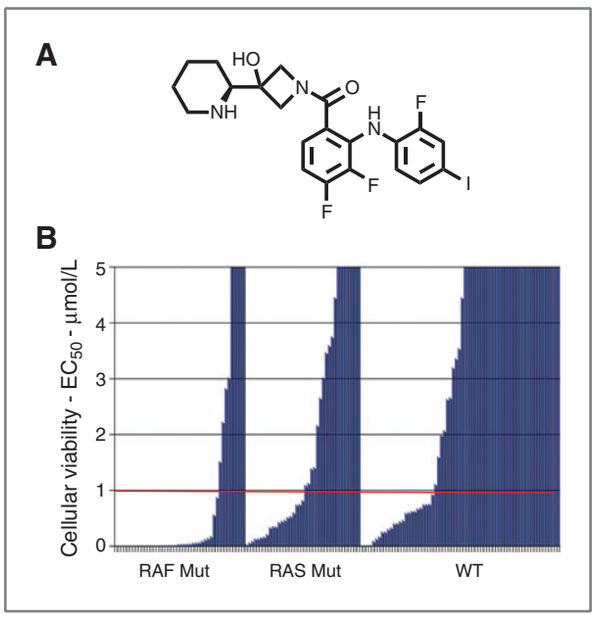

Figure 1. GDC-0973 is a selective, potent MEK inhibitor with efficacy in BRAF and RAS mutant cell lines. A, chemical structure of GDC-0973. B, GDC-0973 was tested in a panel of cell lines in 96-hour viability assays. Relative EC_{50} values are plotted, and cell lines are grouped by RAF and RAS mutation (Mut) status. RAF mutant cell lines include those carrying V600E and other BRAF mutations. RAS mutant cell lines carry mutations in codons 12, 13, or 61 of KRAS or NRAS. All other lines are listed as wild-type (WT). Specific mutations for each cell line are listed in Supplementary Table S2.

Published OnlineFirst November 14, 2011; DOI: 10.1158/0008-5472.CAN-11-1515

MEK1. In biochemical assays, GDC-0973 showed more than 100-fold selectivity for MEK when tested against a panel of more than 100 serine–threonine and tyrosine kinases (Supplementary Table S1).

GDC-0973 shows strong cellular potency in a broad panel of tumor types, particularly in BRAF or KRAS mutant cancer cell lines (Fig. 1B; Supplementary Table S2). In a panel of cancer cell lines, 80% of BRAF mutant lines (including V600E and non-V600E mutations) were sensitive to GDC-0973, 54% of lines carrying oncogenic mutations in *KRAS* or *NRAS* were sensitive, and 35% of the remaining lines were sensitive. As not all RAF and RAS mutant lines are sensitive to MEK inhibition, and not all wild-type lines are resistant, there are clearly additional genetic factors affecting sensitivity and resistance to MEK inhibition.

GDC-0941 is a potent inhibitor of class I PI3K isoforms with biochemical IC_{50} values of 3 to 75 nmol/L for the 4 class I isoforms of PI3K (14). This compound shows excellent selectivity against mTOR, DNA-dependent protein kinase (DNA-PK), and a panel of more than 228 kinases (14). GDC-0941 shows strong inhibition of tumor cells *in vitro* and *in vivo*, especially those with activated PI3K pathway signaling (21). In this cell line panel, 63% of cancer cell lines with oncogenic mutations in *PIK3CA* were sensitive to GDC-0941 (Supplementary Table S2). A higher percentage of RAF and RAS mutant cell lines are resistant to GDC-0941 than RAF and RAS wild-type cell lines (Supplementary Fig. S1).

GDC-0973 has antitumor efficacy in BRAF and KRAS mutant human xenograft tumor models

GDC-0973 showed activity in a number of human tumor xenograft models, particularly in models mutant for BRAF. Two dose-ranging efficacy studies in BRAF mutant and KRAS mutant human xenograft models are shown in Fig. 2. In the A375.X1 $BRAF^{V600E}$ mutant melanoma xenograft model, treatment with doses of GDC-0973 above 3 mg/kg led to strong TGI (Fig. 2A). In the NCI-H2122 $KRAS^{G12C}$ mutant non–small cell lung carcinoma (NSCLC) xenograft model, treatment with up to 5 mg/kg GDC-0973 led to moderate TGI and at 10 mg/kg approached tumor stasis (Fig. 2B). GDC-0973 was tested in additional xenograft tumors with different genetic backgrounds and showed varying degrees of TGI across tumor types and genotypes (Table 1). There was a high degree of sensitivity to GDC-0973 in $BRAF^{V600E}$ mutant melanoma

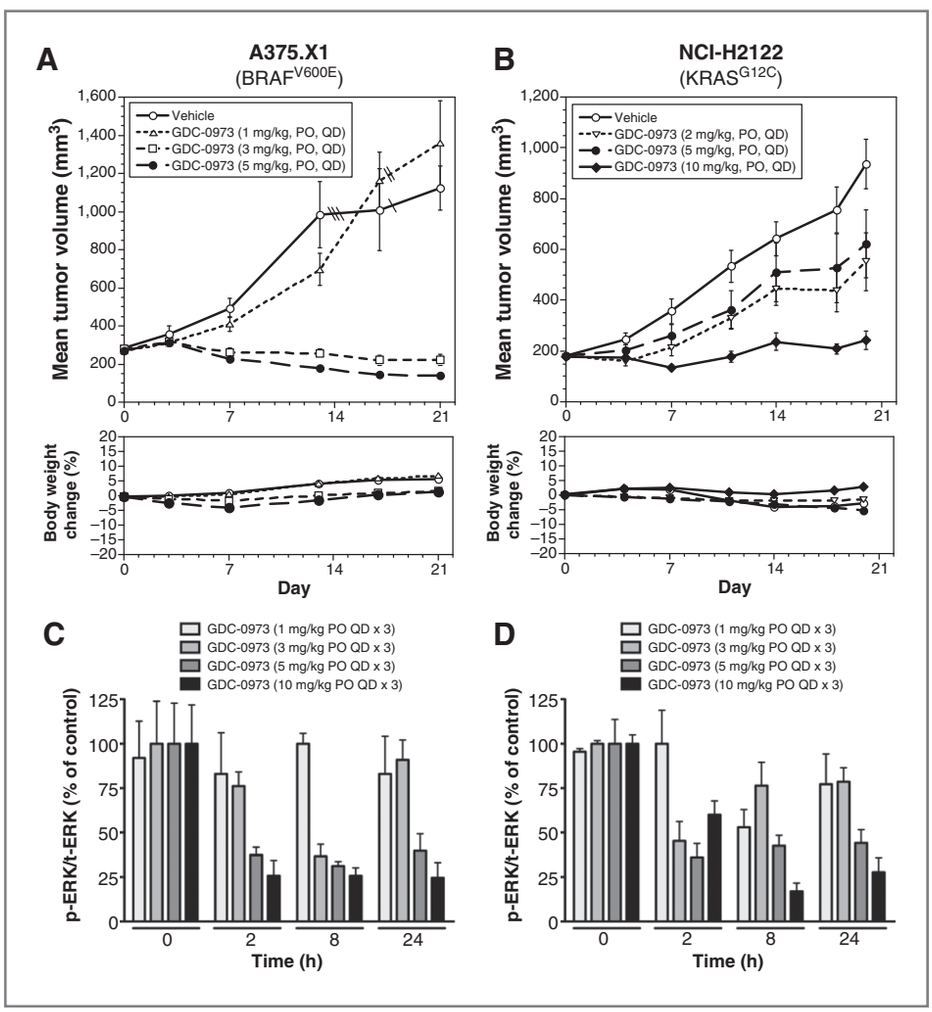

Figure 2. GDC-0973 single-agent efficacy and pharmacodynamic (PD) studies in $BRAF^{V600E}$ and KRAS mutant tumor models. Dose-ranging efficacy studies were carried out in the (A) A375.X1 and (B) NCI-H2122 tumor xenograft models. GDC-0973 was dosed orally daily (QD) for 21 consecutive days. Group mean tumor volumes and SEM are shown. Animals taken off study are indicated with a slash mark. Percentage of body weight change is shown in the bottom. Percentage of tumor growth inhibition (%TGI) is listed in the Supplementary Table S3. A, in the A375.X1 model, 87% TGI was observed at 3 mg/kg and 106% TGI was observed at 5 mg/kg. B, in the NCI-H2122 model, 49% TGI was observed at 5 mg/kg, which approached stasis at 80% TGI at 10 mg/kg. Dose ranging PD studies were conducted in the (C) A375.X1 and (D) NCI-H2122 models in which GDC-0973 was dosed at 1, 3, 5, and 10 mg/kg, QD × 3 days. Tumor phospho- and total-ERK-1/2 (p-ERK and t-ERK, respectively) was quantified by Western blotting as described in Materials and Methods and shown in Supplementary Fig. S2.

Published OnlineFirst November 14, 2011; DOI: 10.1158/0008-5472.CAN-11-1515

Table 1. Summary of single-agent activity of GDC-0973 in human xenograft tumors in mice by %TGI

			Dose, mg/kg		
Xenograft line	**Tissue type**	**Mutation status**	**2.5**	**5**	**10**
Molm-13	AML	FLT3^{Y599_D600insFDFREYE}, c-Cbl^{E366_Q409del}		−6	36
Molm-16	AML	FLT3^{T227M}	7	30	
MX-1	Breast	PTEN^{null}		26	
DLD-1	CRC	KRAS^{G13D}, IDH1^{G97D}, SMO^{T640A}, APC^{I1417fs*2}		50.2_5	49.5_2
HCT-116	CRC	KRAS^{G13D}, PIK3CA^{H1057R}, CTNNB1^{S45del}, CDKN2A^{G23fs}	34	68.7_3	84.5_2
HM7	CRC				37
LoVo	CRC	KRAS^{G13D}, CDKN2A^{P48L}, FBXW7^{R505C}, MSH2$^{?}$, SMO$^{G16_L17insLL,\ A324T}$, NF1$^{R1276Q,\ Y1607fs*17}$, APC$^{1114*,\ M1431fs*42}$		73	98
FaDu	HNSCC	SMAD4^{del}, TP53^{R248L,del}, CDKN2A^{del}	4	94	
537MEL	Melanoma	PTEN^{null}	69	94	96
A2058	Melanoma	BRAF^{V600E}, PTEN$^{L112Q,\ V175fs*3}$, TP53^{V274F}		12.7_3	47.3_3
A2058-X1	Melanoma	BRAF^{V600E}, PTEN$^{L112Q,\ V175fs*3}$, TP53^{V274F}	36	45_2	61
A375	Melanoma	BRAF^{V600E}, CDKN2A^{E61*}	98	120_2	122
A375.X1	Melanoma	BRAF^{V600E}, CDKN2A^{E61*}	97.5_2	106_5	104_2
A427	NSCLC	KRAS^{G12V}, LKB1^{del}, CDKN2A^{del}, CTNNB1^{T41A}, SMARCA4^{del}		-137_2	
A549	NSCLC	KRAS^{G12S}, LKB1^{Q37*}, SMARCA4^{Q729fs*4}, CDKN2A^{del}		51.4_7	108
Calu-6	NSCLC	KRAS^{Q61K}, TP53^{R196*}	27.5_2	80	44
EBC-1	NSCLC	MET^{amp}, EGFR$^{G719S,L858R\ (sub\text{-}population)}$		7	40
NCI-H441	NSCLC	KRAS^{G12V}, TP53^{R158L}, Met^{high}		59	85
NCI-H2122	NSCLC	KRAS^{G13C}, LKB1^{P281fs*6}, TP53^{Q61L,C176FI}, CDKN2A^{del}		49_4	80
NCI-H460	NSCLC	KRAS^{Q61H}, PIK3CA^{E545K}, LKB1^{Q37*}, CDKN2A^{del}	32	34.5_2	9
NCI-H520.X1	NSCLC	TP53^{W146*}, CDKN2A^{G45fs*}		26	21
SKOV-3	Ovarian	FBXW7^{R505L}, CDKN2A^{del}	36	69	63
KP4-X1.1	Pancreatic	KRAS^{G12D}		69.5_2	
MiaPaCa-2	Pancreatic	KRAS^{G12C}, NOTCH1^{L2458V}		6	12
22Rv1	Prostate	PIK3CA^{Q546R}, TP53^{Q331R}		106	82.5_2
DU-145.X1	Prostate	KRAS^{G12V}, LKB1^{K178fs*86}, TP53^{P223L,V274F}, CDKN2A^{del}, MLH1^{del}, SMARCA4^{del}, NF1^{P2472H}, RB1^{K715*}			77
NCI-H69	SCLC	RB1^{E748*}, PIK3CA^{G106_R108del}, TP53^{E171*}		21	38

NOTE: Subscript numbers indicates that the value is average by that number of studies.

tumor models, with strong tumor inhibition often observed at low doses and regression at high doses. An exception was the A2058 BRAF mutant model, where the loss of PTEN may be a resistance factor (8). Apart from BRAF^{V600E} mutant models, there was no strict correlation of tumor inhibition with genotype. In particular, maximal tumor inhibition for KRAS mutant models ranged from 9% to 108% and tumor inhibition in KRAS wild-type models ranged from 21% to 96%, again suggesting that additional genetic factors contribute to the sensitivity to single-agent MEK inhibition.

Pharmacodynamic studies were conducted using the A375.X1 and NCI-H2122 xenograft models in which mice were treated with 3 daily doses of GDC-0973 at 1, 3, 5, or 10 mg/kg. Tumor samples were collected at 2, 8, and 24 hours post last dose and analyzed for p-ERK1/2 and t-ERK1/2 levels. Band intensities were quantified and plotted relative to vehicle-treated mice (time: 0 h). In the A375.X1 model, dose- and time-dependent suppression of p-ERK was observed, with the 10 mg/kg dose of GDC-0973 suppressing p-ERK 75% at 2, 8, and 24 hours (Fig. 2C, Supplementary Fig. S2). In the NCI-H2122 model, GDC-0973 inhibited p-ERK 83% at 8 hours and 73% at 24 hours (Fig. 2D, Supplementary Fig. S2). Lower doses of GDC-0973 showed weaker suppression of p-ERK over time and dose dependency consistent with the single-agent antitumor activity of GDC-0973 in the A375.X1 and NCI-H2122 models, respectively.

GDC-0973 combined with the PI3K inhibitor GDC-0941 causes apoptosis that is mediated in part by Bim

Continuous, simultaneous exposure to GDC-0973 and GDC-0941 resulted in dramatic loss of tumor cell viability relative to patient-matched normal cells *in vitro* (Fig. 3A; Supplementary Fig. S3). GDC-0941 and GDC-0973 were tested for their *in vitro* combination efficacy in a panel of melanoma cell lines by a

Published OnlineFirst November 14, 2011; DOI: 10.1158/0008-5472.CAN-11-1515

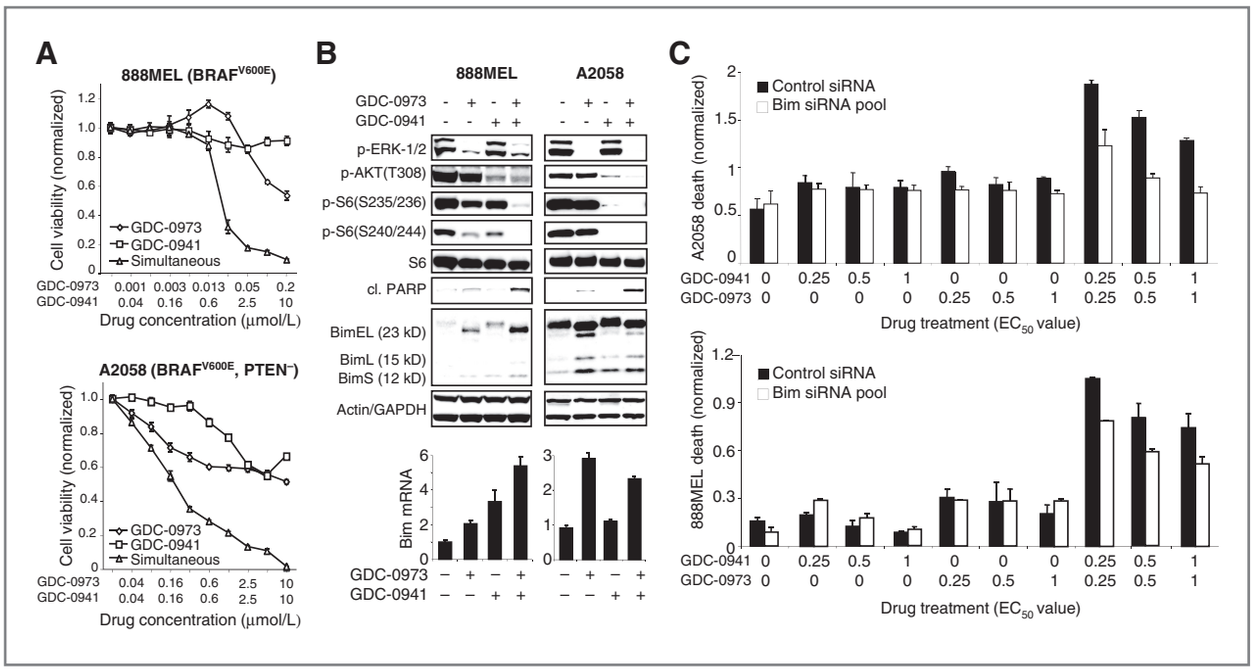

Figure 3. Combination of GDC-0973 + GDC-0941 results in reduced viability, pathway inhibition, and increased apoptosis. A, the 888MEL and A2058 BRAF mutant melanoma cell lines were treated with increasing concentrations of GDC-0973 and GDC-0941 as single agents and in combination and assayed in a 96-hour viability assay. The highest drug concentrations corresponded to 4× EC_{50} doses for 888MEL (0.2 μmol/L GDC-0973, 10 μmol/L GDC-0941) and A2058 (10 μmol/L GDC-0973, 10 μmol/L GDC-0941) cells. B, top, melanoma cells were treated with 1× half maximal effective concentration (EC_{50}) concentration of MEK and PI3K inhibitors for 24 hours (888MEL: 0.05 μmol/L GDC-0973, 2.5 μmol/L GDC-0941; A2058: 2.5 μmol/L GDC-0973, 2.5 μmol/L GDC-0941), and protein lysates were analyzed by immunoblotting. Bottom, RNA was extracted from the melanoma cells treated with 1× EC_{50} drug concentration for 16 hours and analyzed by TaqMan gene expression assay. Bim RNA levels are normalized to GAPDH. C, A2058 cells were treated with distinct siRNA oligonucleotide pools to Bim for 72 hours and subsequently treated for 24 hours with the indicated concentrations of GDC-0941 or GDC-0973 and analyzed by the Cell Death Detection ELISA assay. Differences in cell death induction by GDC-0973 and GDC-0941 combination in the presence or absence of Bim were statistically significant ($P < 0.05$).

4-day CellTiter-Glo viability assay. GDC-0941 and GDC-0973 act cooperatively to inhibit the viability of all melanoma cell lines tested, 60% of which carry oncogenic mutations in BRAF (Supplementary Fig. S4 and Supplementary Table S2). GDC-0941 and GDC-0973 were also tested in a panel of NSCLC cell lines. Because the compounds showed efficacy as single agents in most of the NSCLC cell lines, synergy could be assessed in these lines with Calcusyn, a program using the Chou and Talalay combination index (CI) method for calculating the level of synergy (20). Strong synergy or synergy, as indicated by CI values less than or equal to 0.3 or 0.3 to 0.7, respectively, was observed for 74% ($n = 35$ of 47) of NSCLC cell lines, of which approximately half carry oncogenic mutations in KRAS (Supplementary Table S2). The remaining 26% of lung cancer cell lines could not be evaluated for synergy because one of the compounds showed no efficacy as a single agent. There was no statistically significant genotype dependence of combination efficacy with respect to BRAF or KRAS mutation status in the cell lines tested.

The effects of combined MEK and PI3K pathway inhibition on downstream pathway markers were evaluated in cell lines. Analysis of downstream pathway markers in the 888MEL (BRAF V600E) and A2058 (BRAFV600E) mutant melanoma cell lines showed that treatment with GDC-0973 decreased p-ERK whereas treatment with GDC-0941 decreased p-AKT in these cell lines (Fig. 3B). Whereas GDC-0941 was able to decrease phosphorylation of ribosomal protein S6 (pS6) moderately on its own, pS6 showed greater decrease in response to the combination at both the S235/236 and S240/244 sites in multiple tumor cell lines (Fig. 3B, Supplementary Fig. S5A). The single agent and combination treatments were also assessed for their effect on apoptotic markers. Treatment with GDC-0973 and GDC-0941 resulted in a combinatorial increase of cellular mediators of apoptosis, such as cleaved PARP and alternatively spliced isoforms of Bim (Fig. 3B; ref. 19). The majority of cell lines tested showed a stronger response of Bim to GDC-0973 than to GDC-0941, whereas the increase in cleaved PARP was equally dependent on both compounds (Fig. 3B, Supplementary Fig. S5A), suggesting additional apoptotic mechanisms are involved. Consistent with expectations based on the published literature (22, 23), combined GDC-0973 and GDC-0941 treatment increased Bim levels via several complementary mechanisms, including gene expression, BimEL phosphorylation, and Bim protein stabilization. Decreases of pS6 and Bim in tumors were also observed *in vivo* in response to the combination (Supplementary Fig. S5B and S5C). To confirm the functional contribution of Bim in mediating apoptosis induced by MEK and PI3K inhibition, RNA interference studies were conducted to ablate Bim in melanoma cells (Fig. 3C; Supplementary Fig. S6A and S6B). In

Published OnlineFirst November 14, 2011; DOI: 10.1158/0008-5472.CAN-11-1515

the presence of increasing concentrations of GDC-0973 and GDC-0941, selective knockdown of Bim significantly attenuated cell death induced by MEK and PI3K blockade in A2058 melanoma cells (Fig. 3C).

GDC-0973 and GDC-0941 show improved efficacy in combination in BRAF and KRAS mutant xenograft models *in vivo*

Similar to *in vitro* combination results, the combination of GDC-0973 and GDC-0941 showed increased efficacy compared with single-agent treatment in multiple human xenograft tumor models (Fig. 4A–D). Four xenograft tumor models harboring BRAF or KRAS mutations with or without alterations in PTEN or PIK3CA were evaluated for response to GDC-0973 and GDC-0941 as single agents and in combination. For the A2058 ($BRAF^{V600E}$, $PTEN^{-}$), DLD-1 ($KRAS^{G13D}$, $PIK3CA^{E545K}$), and NCI-H2122 ($KRAS^{G12C}$) models, doses of GDC-0973 and GDC-0941 were selected to produce moderate single-agent activity in each model to visualize improvement of efficacy in the combination arms. For the A375 ($BRAF^{V600E}$) model, all tested doses of GDC-0973 showed regression and all tested doses of GDC-0941 showed lack of TGI, however, the combination of GDC-0973 and GDC-0941 led to a greater tumor response rate as GDC-0973 resulted in 70% (7/10) complete responses (CR), whereas the combination resulted in 100% (10/10) CRs. As a result, upon cessation of treatment, tumors were slower to grow back in the combination arm versus the GDC-0973 single-agent arm (Fig. 4A). In A2058 (Fig. 4B), DLD-1 (Fig. 4C), and NCI-H2122 (Fig. 4D), combination of GDC-0973 and GDC-0941 resulted in stronger tumor suppression than either single agent alone in all models tested (summarized in Supplementary Table S3). These results show that the combination activity observed *in vitro* translates into increased combined antitumor efficacy *in vivo*. Combination

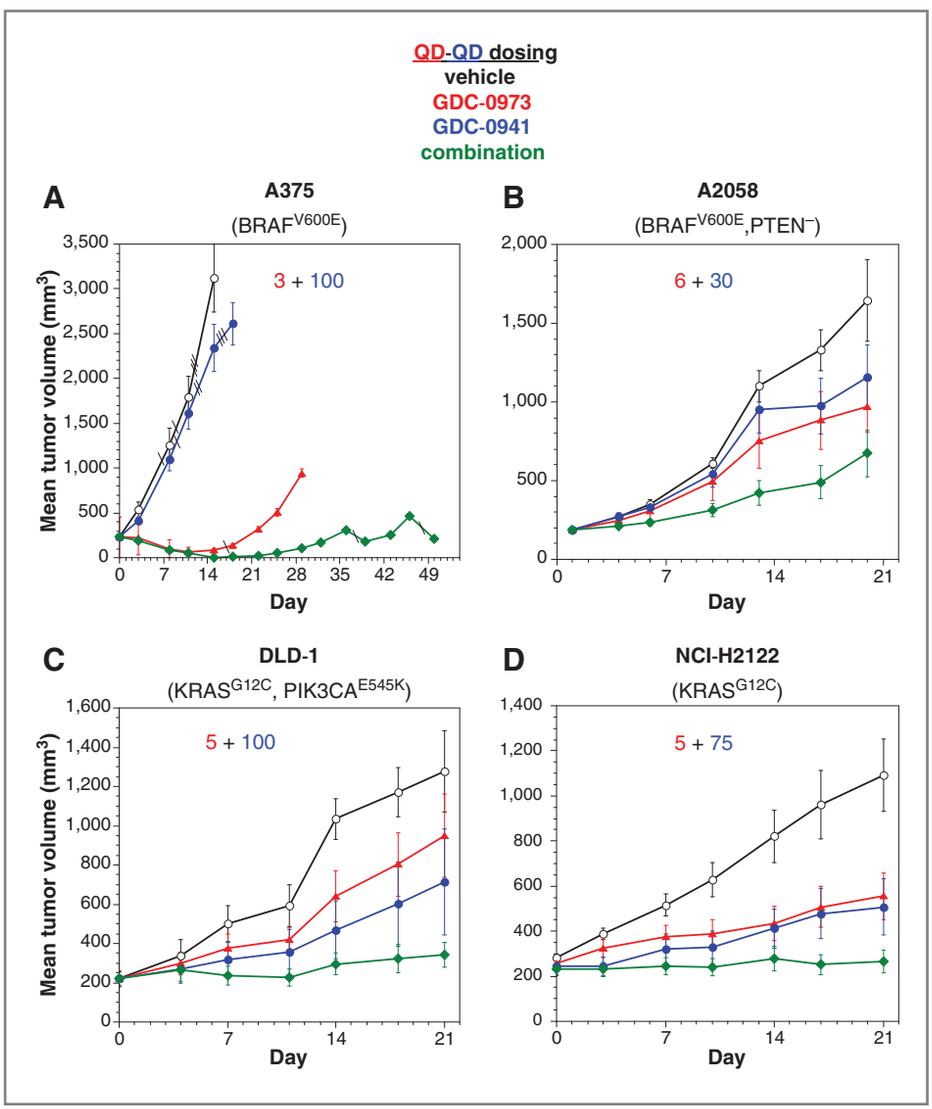

Figure 4. GDC-0973 and GDC-0941 combination results in TGI when dosed daily. *In vivo* combination efficacy studies were run in 4 tumor xenograft models: (A) A375 ($BRAF^{V600E}$), (B) A2058 ($BRAF^{V600E}$, $PTEN^{-}$), (C) DLD-1 ($KRAS^{G13D}$, $p110\alpha^{E545K}$), and (D) NCI-H2122 ($KRAS^{G12C}$). Group mean tumor volumes and SEM is shown. Animals taken off study are indicated with a slash mark. Vehicle (black open circles and lines), GDC-0973 (red triangles and lines), GDC-0941 (blue circles and lines), or a combination of the 2 drugs (green diamonds and lines) were dosed orally, daily (QD) for 21 consecutive days at the indicated doses labeled in the panels. Percentage of TGI is listed in the Supplementary Table S3. In the A375 study, mice treated with single agent GDC-0973 had a 70% CR rate whereas mice treated with the combination had a 100% CR rate.

Published OnlineFirst November 14, 2011; DOI: 10.1158/0008-5472.CAN-11-1515

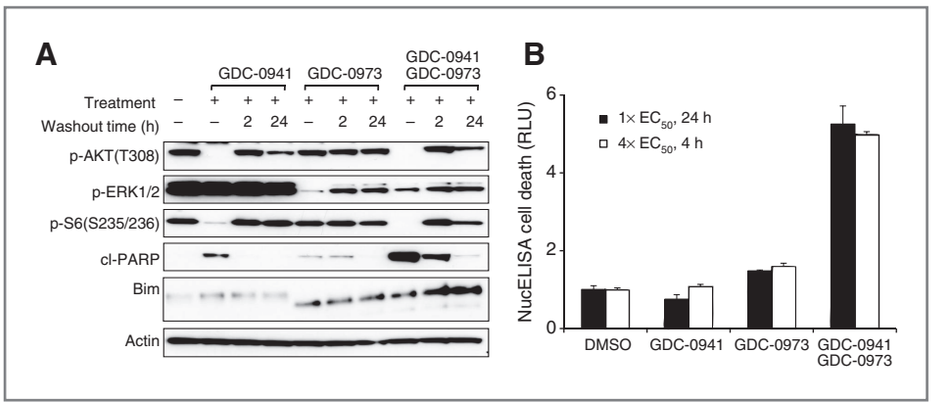

Figure 5. Transient treatment of GDC-0973 + GDC-0941 results in apoptosis and prolonged accumulation of Bim. A, 888MEL cells were treated with 0.05 μmol/L GDC-0973 and 5 μmol/L GDC-0941 as single agents or in combination for 24 hours and then washed to remove the compounds. Lysates were made at subsequent time points after washout (2 and 24 hours) and analyzed by immunoblotting. B, 888MEL cells were treated with a 1× EC_{50} concentration of GDC-0973 and/or GDC-0941 for 24 hours or a 4× EC_{50} concentration for 4 hours prior to exchanging media to remove the compounds. Cells were analyzed at the 24 hour time point for apoptosis by the Cell Death Detection ELISA assay. cl-PARP, cleaved PARP; DMSO, dimethyl sulfoxide.

pharmacokinetic studies showed that there were no drug–drug interactions that impacted the exposure of either compound (E.F. Choo, submitted for publication).

Transient exposure to MEK and PI3K inhibitors results in apoptosis

Given that exposure to GDC-0973 and GDC-0941 resulted in apoptosis, we hypothesized that transient inactivation of MEK and PI3K signaling could be sufficient to elicit antitumor efficacy. To examine this possibility, 888MEL cells were pretreated with GDC-0973, GDC-0941, or both for 24 hours followed by washout of compounds and serial evaluation of downstream markers over time (Fig. 5A). After treatment with single agent GDC-0941, the proximal pathway markers p-AKT and pS6 were strongly inhibited but rapidly returned to baseline levels within 2 hours following washout. Treatment with single agent GDC-0973 resulted in a strong decrease of p-ERK that only partially rebounded after washout. Transient treatment with the combination had identical effects on p-ERK, p-AKT, and pS6 as the single agents. However, there was a combined enhancement of Bim protein accumulation and cleaved PARP. Bim protein levels were modestly increased above baseline in response to single agent GDC-0973 and were maintained for 24 hours after compound washout. This increase was more pronounced in response to combination treatment. Cleaved PARP was modestly induced in response to single-agent treatment with GDC-0973 or GDC-0941. It was more strongly increased in response to the combination, although it did not persist through 24 hours after washout. This is perhaps due to detachment of late apoptotic cells from the plates during repeated wash cycles.

To confirm the functional consequences of transient exposure to GDC-0973 and GDC-0941, cell death was assessed by a nucleosomal ELISA apoptosis assay. Transient treatment of 888MEL cells with either single agent GDC-0973 or GDC-0941 resulted in minimal to no apoptosis induction, whereas GDC-0973 plus GDC-0941 resulted in a 5-fold increase in apoptosis (Fig. 5B). A comparable extent of apoptosis was observed for cells that were exposed to either a low concentration of the inhibitors for 24 hours or a high concentration for 4 hours. Effects of transient combination treatment on cell proliferation were also observed (Supplementary Fig. S7A and S7B). To confirm these results *in vivo*, mice bearing A2058 xenograft tumors were dosed daily with GDC-0941 and GDC-0973 for 4 days, and then tumors were excised and analyzed serially after the last dose. As expected, pS6 levels returned to baseline by 8 hours after the final dose (Supplementary Fig. S7C). Taken together, these results show that continuous pathway suppression is not necessary to elicit sustained effects on proliferation and apoptosis.

Intermittent dosing of MEK and PI3K inhibitors is efficacious *in vivo*

The cell washout studies producing apoptosis suggested that continuous exposure to the combination of GDC-0973 and GDC-0941 is not required for efficacy. This was tested in the A375.X1, A2058, DLD-1, and NCI-H2122 xenograft tumor models by dosing both GDC-0973 and GDC-0941 on an every third day intermittent schedule (Fig. 6A–D). Each tumor model varied in its sensitivity to the 2 compounds, and doses were chosen to produce modest single-agent activity. When both drugs were dosed intermittently on an every third day regimen increased TGI was observed in response to the combination in all 4 models. While all the models showed some degree of improvement of efficacy in combination, tumor inhibition of the combination differed most from single-agent activity in the DLD-1 colon cancer xenograft model, which carries mutations in both KRAS and PIK3CA.

Pharmacodynamic studies were conducted in the A2058 xenograft model to assess the response of downstream markers to intermittent dosing with GDC-0973 and GDC-0941. Briefly, both GDC-0973 and GDC-0941 were administered intermittently every third day for a total of 2 doses at 15 and 150 mg/kg, respectively. Tumors were harvested at 8 and 72 hours following the second dose and analyzed by Western blotting for various downstream pathway markers.

Published OnlineFirst November 14, 2011; DOI: 10.1158/0008-5472.CAN-11-1515

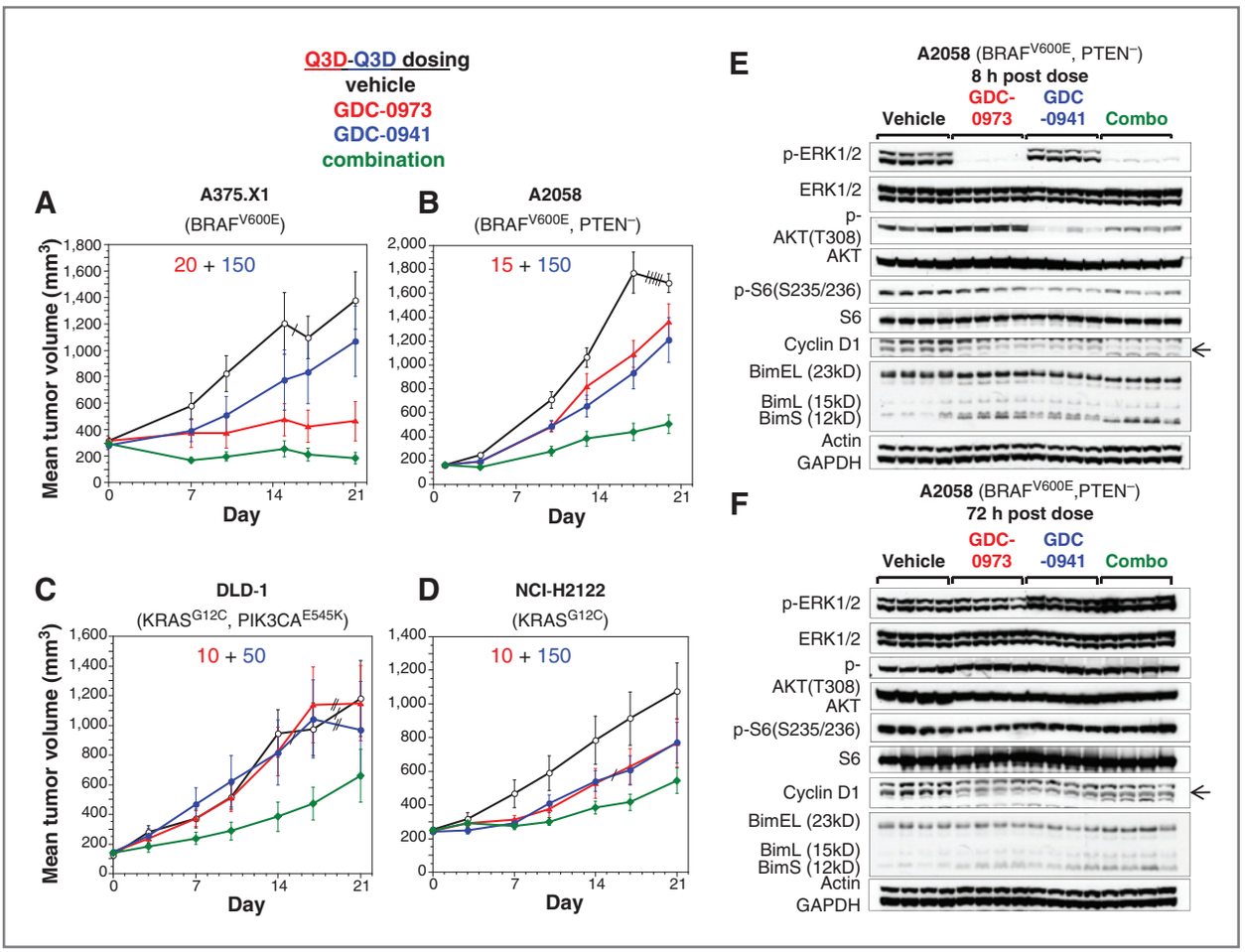

Figure 6. GDC-0973 and GDC-0941 combination results in TGI when dosed intermittently. *In vivo* combination efficacy studies were run in 4 tumor xenograft models: (A) A375.X1 ($BRAF^{V600E}$), (B) A2058 ($BRAF^{V600E}$, $PTEN^{-}$), (C) DLD-1 ($KRAS^{G13D}$, $p110\alpha^{E545K}$), and (D) NCI-H2122 ($KRAS^{G12C}$). Group mean tumor volumes and SEM is shown. Animals taken off study are indicated with a slash mark. Vehicle (black open circles and lines), GDC-0973 (red triangles and lines), GDC-0941 (blue circles and lines), or a combination (Combo) of the 2 drugs (green diamonds and lines) were dosed orally, every third day (Q3D) for 21 consecutive days at the indicated doses labeled in the panels. Percentage of TGI is listed in Supplementary Table S3. Tumor PD studies were conducted in the A2058 xenograft tumor model at 8 hours (E) and 72 hours (F) post last dose. Briefly, tumor-bearing mice were treated for a total of 2 doses of GDC-0973 and GDC-0941 at 15 and 150 mg/kg, respectively, both given Q3D. Multiple downstream response markers were assessed by Western blotting.

At 8 hours post last dose, intermittent GDC-0973 treatment resulted in robust suppression of p-ERK, a mild decrease in cyclin D1 levels, and an increase in BimS and BimL levels (Fig. 6E). GDC-0941 treatment resulted in suppression of p-AKT with a modest decrease in phospho-S6 levels, as well as a slight increase in BimS and BimL levels (Fig. 6E). Combination treatment resulted in a more pronounced decrease in cyclin D1 levels at 8 hours as well as a stronger induction of BimS levels (Fig. 6E). Mobility of the BimS, BimL, and BimEL isoforms was increased, consistent with a more stable and dephosphorylated form of Bim (Fig. 3B; refs. 22, 23). At 72 hours post last dose, p-ERK, p-AKT, and pS6 levels had returned to baseline levels in both single agent and combination-treated tumors (Fig. 6F). However, cyclin D1 levels remained lower and Bim levels remained slightly elevated in response to combination treatment. This is consistent with intermittent pathway knockdown resulting in more sustained effects on downstream markers of proliferation and apoptosis.

Similar intermittent efficacy was observed using a different PI3K inhibitor, GDC-0980, when dosed daily or once a week in combination with GDC-0973 (Supplementary Fig. S8A and S8B). Combination efficacy has also been published with a different MEK inhibitor, PD0325901, when dosed intermittently with GDC-0941 (15). Therefore, intermittent efficacy with MEK and PI3K inhibitors has observed with multiple inhibitors.

Discussion

In the past several years, there have been numerous studies published on combinations of targeted agents in preclinical cancer models, and more recently, combinations of novel targeted agents have begun to be tested in the clinic

Published OnlineFirst November 14, 2011; DOI: 10.1158/0008-5472.CAN-11-1515

(24, 25). For inhibitors of the PI3K and MEK pathways, there are currently more than half a dozen phase Ib combination trials in progress combining selective targeted agents against nodes in these pathways (26–29). There are many important questions to be addressed including which nodes in the pathways will be most efficacious and best tolerated in combination, identifying which patients will be most likely to benefit from a particular combination, and which doses and schedules will be optimal for efficacy and tolerability.

Dose and schedule selection can be affected by both the pharmacokinetic profile and *in vivo* mechanism of combination activity of the 2 agents. For the selective MEK inhibitor GDC-0973 and class I PI3K inhibitor GDC-0941, the mechanism of combination activity was shown to be synergistic regulation of cap-dependent translation (pS6, p4E-BP1), cell-cycle progression (cyclin D1, $p27^{Kip1}$), and cellular apoptosis (Figs. 3 and 5; ref. 30). MEK/PI3K-dependent apoptosis was showed by increased cleavage of PARP and mediated at least in part through increased levels of the proapoptotic Bim protein. Complete rescue of apoptosis was not observed in Bim loss-of-function experiments and this may be due to additional MEK and PI3K effectors that also contribute to survival signaling by these pathways (30–32).

Given that the effects on knock-down of downstream markers have typically been evaluated in cells under constant exposure to compound (33, 34), we tested how transient exposure to GDC-0973 plus GDC-0941 would affect the time course of downstream pathway inhibition and recovery. Whereas the majority of pathway markers returned to baseline levels within 2 hours after removal of the compounds, Bim remained elevated up through 24 hours after compound removal, showing a sustained elevation of apoptotic activity.

These findings translated *in vivo*, where pharmacodynamic data show that pS6 levels in tumors returned to baseline by 8 to 24 hours after dosing with GDC-0973 + GDC-0941, indicating recovery of MAPK and PI3K pathway signaling at efficacious doses. Previous data have shown a similar time course for recovery of the p-AKT signaling pathway after treatment with GDC-0941 (33). The fact that the every 3 day schedule is efficacious suggests that continuous pathway knock-down is not required for TGI, as the compounds are cleared from the system and proximal pathway signaling returned to normal for more than 24 hours prior to the next dose.

The every 3 day schedule used in these studies is a proof of concept that intermittent dosing can be efficacious and is not suggestive that this is the optimal schedule to be used preclinically or clinically. Several factors will affect the optimal dose and schedule of a combination in the clinic (35). After gaining understanding of the mechanism of combination efficacy, the half-life of each of the compounds must be considered, which differ substantially between mice and humans. The schedule may also be affected by tolerability, thereby affecting the therapeutic index. The pharmacokinetic drivers of efficacy and toxicity may be different and are being assessed by MEK and PI3K pathway inhibitor combination trials, including GDC-0973 and GDC-0941. With efficacy in BRAF and KRAS mutant preclinical models achieved with both continuous and intermittent schedules, it generates multiple paths for clinical investigation.

Disclosure of Potential Conflicts of Interest

K.P. Hoeflich, M. Merchant, C. Orr, J. Chan, D. Den Otter, L. Berry, I. Kasman, H. Koeppen, L.S. Friedman, and M. Belvin are employees of Genentech, Inc. S. Engst, S. Johnston, and K. Rice are or were employees of Exelixis, Inc. No potential conflicts of interest were disclosed by the other author.

Acknowledgments

The authors thank Georgia Hatzivassiliou, Bonnie Liu, Rich Neve, Klara Totpal, the IVCC group, Jason Boggs, and our immunohistochemistry staff for providing insightful discussions, suggestions, and technical assistance.

The costs of publication of this article were defrayed in part by the payment of page charges. This article must therefore be hereby marked *advertisement* in accordance with 18 U.S.C. Section 1734 solely to indicate this fact.

Received May 5, 2011; revised October 19, 2011; accepted November 6, 2011; published OnlineFirst November 14, 2011.

References

1. Downward J. Targeting RAS signalling pathways in cancer therapy. Nat Rev Cancer 2003;3:11–22.
2. Roberts PJ, Der CJ. Targeting the Raf-MEK-ERK mitogen-activated protein kinase cascade for the treatment of cancer. Oncogene 2007;26:3291–310.
3. Wellbrock C, Karasarides M, Marais R. The RAF proteins take centre stage. Nat Rev Mol Cell Biol 2004;5:875–85.
4. Solit DB, Garraway LA, Pratilas CA, Sawai A, Getz G, Basso A, et al. BRAF mutation predicts sensitivity to MEK inhibition. Nature 2006;439:358–62.
5. Hoeflich KP, Jaiswal B, Davis DP, Seshagiri S. Inducible BRAF suppression models for melanoma tumorigenesis. Methods Enzymol 2008;439:25–38.
6. Bamford S, Dawson E, Forbes S, Clements J, Pettett R, Dogan A, et al. The COSMIC (Catalogue of Somatic Mutations in Cancer) database and website. Br J Cancer 2004;91:355–8.
7. Davies H, Bignell GR, Cox C, Stephens P, Edkins S, Clegg S, et al. Mutations of the BRAF gene in human cancer. Nature 2002;417:949–54.
8. Hoeflich KP, Herter S, Tien J, Wong L, Berry L, Chan J, et al. Antitumor efficacy of the novel RAF inhibitor GDC-0879 is predicted by BRAFV600E mutational status and sustained extracellular signal-regulated kinase/mitogen-activated protein kinase pathway suppression. Cancer Res 2009;69:3042–51.
9. Ward S, Sotsios Y, Dowden J, Bruce I, Finan P. Therapeutic potential of phosphoinositide 3-kinase inhibitors. Chem Biol 2003;10:207–13.
10. Cantley LC. The role of phosphoinositide 3-kinase in human disease. Harvey Lect 2004;100:103–22.
11. Bachman KE, Argani P, Samuels Y, Silliman N, Ptak J, Szabo S, et al. The PIK3CA gene is mutated with high frequency in human breast cancers. Cancer Biol Ther 2004;3:772–5.
12. Samuels Y, Velculescu VE. Oncogenic mutations of PIK3CA in human cancers. Cell Cycle 2004;3:1221–4.
13. Karakas B, Bachman KE, Park BH. Mutation of the PIK3CA oncogene in human cancers. Br J Cancer 2006;94:455–9.
14. Folkes AJ, Ahmadi K, Alderton WK, Alix S, Baker SJ, Box G, et al. The identification of 2-(1H-indazol-4-yl)-6-(4-methanesulfonyl-piperazin-1-ylmethyl)-4-morpholin-4-yl-thieno[3,2-d]pyrimidine (GDC-0941) as

Published OnlineFirst November 14, 2011; DOI: 10.1158/0008-5472.CAN-11-1515

a potent, selective, orally bioavailable inhibitor of class I PI3 kinase for the treatment of cancer. J Med Chem 2008;51:5522–32.
15. Sos ML, Fischer S, Ullrich R, Peifer M, Heuckmann JM, Koker M, et al. Identifying genotype-dependent efficacy of single and combined PI3K- and MAPK-pathway inhibition in cancer. Proc Natl Acad Sci U S A 2009;106:18351–6.
16. Engelman JA, Chen L, Tan X, Crosby K, Guimaraes AR, Upadhyay R, et al. Effective use of PI3K and MEK inhibitors to treat mutant Kras G12D and PIK3CA H1047R murine lung cancers. Nat Med 2008;14:1351–6.
17. Mirzoeva OK, Das D, Heiser LM, Bhattacharya S, Siwak D, Gendelman R, et al. Basal subtype and MAPK/ERK kinase (MEK)-phosphoinositide 3-kinase feedback signaling determine susceptibility of breast cancer cells to MEK inhibition. Cancer Res 2009;69:565–72.
18. Hoeflich KP, O'Brien C, Boyd Z, Cavet G, Guerrero S, Jung K, et al. *In vivo* antitumor activity of MEK and phosphatidylinositol 3-kinase inhibitors in basal-like breast cancer models. Clin Cancer Res 2009;15:4649–64.
19. O'Connor L, Strasser A, O'Reilly LA, Hausmann G, Adams JM, Cory S, et al. Bim: a novel member of the Bcl-2 family that promotes apoptosis. EMBO J 1998;17:384–95.
20. Chou TC, Talalay P. Quantitative analysis of dose-effect relationships: the combined effects of multiple drugs or enzyme inhibitors. Adv Enzyme Regul 1984;22:27–55.
21. O'Brien C, Wallin JJ, Sampath D, GuhaThakurta D, Savage H, Punnoose EA, et al. Predictive biomarkers of sensitivity to the phosphatidylinositol 3′ kinase inhibitor GDC-0941 in breast cancer preclinical models. Clin Cancer Res 2011;16:3670–83.
22. Cragg MS, Jansen ES, Cook M, Harris C, Strasser A, Scott CL. Treatment of B-RAF mutant human tumor cells with a MEK inhibitor requires Bim and is enhanced by a BH3 mimetic. J Clin Invest 2008;118:3651–9.
23. Pinon JD, Labi V, Egle A, Villunger A. Bim and Bmf in tissue homeostasis and malignant disease. Oncogene 2008;27 Suppl 1:S41–52.
24. Dancey JE, Chen HX. Strategies for optimizing combinations of molecularly targeted anticancer agents. Nat Rev Drug Discov 2006;5:649–59.
25. Kummar S, Chen HX, Wright J, Holbeck S, Millin MD, Tomaszewski J, et al. Utilizing targeted cancer therapeutic agents in combination: novel approaches and urgent requirements. Nat Rev Drug Discov 2010;9:843–56.
26. Fremin C, Meloche S. From basic research to clinical development of MEK1/2 inhibitors for cancer therapy. J Hematol Oncol 2009;3:8.
27. Dhomen N, Marais R. BRAF signaling and targeted therapies in melanoma. Hematol Oncol Clin North Am 2009;23:529–45, ix.
28. Cleary JM, Shapiro GI. Development of phosphoinositide-3 kinase pathway inhibitors for advanced cancer. Curr Oncol Rep 2010;12:87–94.
29. Liu P, Cheng H, Roberts TM, Zhao JJ. Targeting the phosphoinositide 3-kinase pathway in cancer. Nat Rev Drug Discov 2009;8:627–44.
30. She QB, Halilovic E, Ye Q, Zhen W, Shirasawa S, Sasazuki T, et al. 4E-BP1 is a key effector of the oncogenic activation of the AKT and ERK signaling pathways that integrates their function in tumors. Cancer Cell 2010;18:39–51.
31. Manning BD, Cantley LC. AKT/PKB signaling: navigating downstream. Cell 2007;129:1261–74.
32. McCubrey JA, Steelman LS, Chappell WH, Abrams SL, Wong EW, Chang F, et al. Roles of the Raf/MEK/ERK pathway in cell growth, malignant transformation and drug resistance. Biochim Biophys Acta 2007;1773:1263–84.
33. Salphati L, Wong H, Belvin M, Bradford D, Edgar KA, Prior WW, et al. Pharmacokinetic-pharmacodynamic modeling of tumor growth inhibition and biomarker modulation by the novel phosphatidylinositol 3-kinase inhibitor GDC-0941. Drug Metab Dispos 2010;38:1436–42.
34. Choo EF, Belvin M, Chan J, Hoeflich K, Orr C, Robarge K, et al. Preclinical disposition and pharmacokinetics-pharmacodynamic modeling of biomarker response and tumour growth inhibition in xenograft mouse models of G-573, a MEK inhibitor. Xenobiotica 2010;40:751–62.
35. Undevia SD, Gomez-Abuin G, Ratain MJ. Pharmacokinetic variability of anticancer agents. Nat Rev Cancer 2005;5:447–58.

Published OnlineFirst November 14, 2011; DOI: 10.1158/0008-5472.CAN-11-1515

Cancer Research
The Journal of Cancer Research (1916–1930) | The American Journal of Cancer (1931–1940)

AACR American Association for Cancer Research

Intermittent Administration of MEK Inhibitor GDC-0973 plus PI3K Inhibitor GDC-0941 Triggers Robust Apoptosis and Tumor Growth Inhibition

Klaus P. Hoeflich, Mark Merchant, Christine Orr, et al.

Cancer Res 2012;72:210-219. Published OnlineFirst November 14, 2011.